The International Journal of Advanced Manufacturing Technology (2022) 121:1639–1650
https://doi.org/10.1007/s00170-022-09351-5

ORIGINAL ARTICLE

Effects of a new filling technique on the mechanical properties of ABS specimens manufactured by fused deposition modeling

Heba Hussam[1] · Yasser Abdelrhman[1] · M.-Emad S. Soliman[1] · Ibrahim M. Hassab-Allah[1]

Received: 25 January 2022 / Accepted: 7 May 2022 / Published online: 1 June 2022

Abstract
The spread of 3D printing in many different fields has become eminent. This paper aims to improve the mechanical properties of parts printed by fused deposition modeling technique. Acrylonitrile butadiene styrene (ABS) specimens are printed with custom printing parameters. These parameters give a tensile strength that is 86% of the injection- molded ABS strength, and give one of the best recorded results for 100% infill printed ABS tensile specimens. Furthermore, a post filling technique has been studied. Specimens are printed with inner voids and different densities using slicing software. Void shape is precisely selected to conform to the filling process. High-strength, low-cost thermoset resin is injected through specimens to fill those voids. A tensile test has been performed after the full curing of the resin. A morphology analysis is done. Using this technique strength to printed weight ratio is improved by 151% and the cost is reduced by 51%.

Keywords Mechanical properties · FDM · Epoxy resin · Filling · Voiding · Injection

Nomenclature

σ_t	Tensile strength
E_t	Elastic modulus
σ_f	Flexural strength
E_f	Flexural modulus

1 Introduction

Additive manufacturing (AM) is the best choice to join the fourth industrial revolution, as it delivers complex and customized products with great freedom in design in a very short time, reducing the production cost, and shortening the development cycle [1–4]. Stereo-lithography (SLA) is the first technique that AM started with, which is a liquid-based raw material technique. Later on, many techniques were invented varying in the raw material from liquid, to powder, and solid [5]. All AM techniques use three-dimensional computer-aided designs (CAD) to produce — layer by layer — three-dimensional products by selectively adding materials, with variety in the materials being used. Fused deposition modeling (FDM), solid-based AM technique, is the most common and widely used technique due to its simplicity and low price as it utilizes low-cost polymers only [5, 6]. FDM feeds thermoplastic filament into a heating chamber until it reaches a semi-liquid state, extrudes it through a nozzle above its melting point, then deposits it on the printing platform in specified positions according to the G-code generated by the machine's software [7]. FDM printed parts have been in use in many fields like rapid prototyping, building, healthcare devices and tools, motor drives, and aerospace components [8]. But due to the nature of the FDM technique, it experiences some drawbacks; one of them is the limitation in mechanical properties. This limitation is due to the weak and non-homogenous bonding between the corresponding layers building up the part and also between the roads building the layer itself. Also, since the cooling and heating rates in FDM are unstable, there would be uncontrolled shrink and defects in the microstructure [5, 9].

Many studies have been performed to overcome the mentioned problems, covering different materials that are currently used in FDM (ABS, PLA, PA, NYLON, etc.). Many studies have considered printing parameters as important indices for product quality. They studied the influence of printing orientation, speed, raster angle, infill pattern, nozzle temperature, and layer height on the mechanical properties of the printed parts [10–12]. Table 1 summarizes the studies

✉ Yasser Abdelrhman
yasser.abdelrhman@aun.edu.eg

Heba Hussam
heba.hussam@eng.au.edu.eg

[1] Mechanical Design and Production Engineering Department, Faculty of Engineering, Assiut University, Assiut 71515, Egypt

Table 1 Previous work on ABS printed specimens

Authors	Parameters and (levels)	Outputs
Samykano et al. [13]	Printing speed (30 mm/s), printing temperature (220 °C), bed temperature (110 °C), infill pattern (lines), layer height (0.35, 0.4, and 0.5 mm), and raster angle (45°, 55°, 65°)	σ_t (33.7 MPa) E_t (787.7 MP) Toughness (2.83 J/m^3)
Rangisetty and Peel [14]	Layer height (0.2 mm), extruder temperature (240 °C), bed temperature (90 °C), print speed (55 mm/s), and infill pattern (line, concentric, triangular, and honeycomb)	σ_t (30.1 MPa) E_t (2133 MPa) σ_f (50.6 MPa) E_f (2122 MPa)
Bamiduro et al. [15]	Orientation (0°/90°, − 45°/45°)	σ_t (29.65 MPa)
Meng et al. [9]	Layer height (0.1 mm), orientation (vertical, horizontal), printing speed (40 mm/s), extruder temperature (235 °C), bed temperature (80 °C), composition (ABS,ABS/SiO_2, ABS/MMT, ABS/MWCNTs, ABS/$CaCO_3$)	σ_t (28 MPa) σ_f (54.8 MPa) E_f (1650 MPa)
Coogan and Kazmer [16]	Bed temperature (100 °C, 125 °C, 150 °C), print speed (1000, 2000, 4000) mm/min, layer height (0.15,0.3,0.45 mm), nozzle temperature (230 °C, 255 °C, 280 °C), fiber width (0.4, 0.6, 0.8 mm)	Bond strength (28 MPa) Longitudinal strength (34.5 MPa)
Huang et al. [17]	Layer thickness(0.1, 0.2, 0.3 mm), raster angle (45°/-45°,30°/-60°, 0°/90°), printing speed (20, 40, 60 mm/s), building orientation (horizontal, lateral, vertical), bed temperature (80 °C), printing temperature (235 °C)	σ_t (33.6 MPa) σ_f (64.4 MPa) Impact strength (18.44 MPa)
Koch et al. [18]	Print temperature (250 °C), bed temperature (210 °C), layer height (0.2 mm), raster angle (0°, −45°/45°, 90°), travel speed (2000 mm/min), solidity ratio (0.6–1)	σ_t (33.8 MPa)
Cantrell et al. [19]	Layer height (0.1 mm), printing temperature (235 °C), bed temperature (105 °C), orientation (Horizontal, lateral, vertical), raster angle (−45°/45°,0°/90°, 30°/−60°,15°/−75°)	σ_t (33.5 MPa)
Rayegani and Onwubolu [20]	Orientation (0°, 90°), raster angle (0°, 45°), raster width (0.2032, 0.558 mm), air gap (0.558, −0.00254 mm)	σ_t (34.07 MPa)

done by researchers on 3D printed ABS parts applying different printing parameters.

Other studies adopted the potential of improving physical and mechanical properties of the raw material itself. Nanoparticles were prepared and mixed with the printing filament to produce a new one [9, 21–23]. Some researches focused on improving the overall mechanical properties of the 3D printed part by decreasing its anisotropy or increasing its isotropic behavior [24, 25]. They replaced the thermoplastic polymers that result in poor chemical and thermal properties with two-component epoxy resin [24], epoxy resin has good chemical and physical properties and gives high-strength bonding, with light weight structures withstanding high static loads [26–28]. Filippova et al. [25] impregnated ABS 3D printed samples in epoxy resin compound with different hardeners. 142% and 133% were achieved as an improvement in ultimate tensile strength depending on the hardener type. Instead of impregnation, Belter and Dollar [29] injected epoxy resin through ABS flexural specimens. This resulted in improving the overall part stiffness and strength up to 25% and 45%, respectively. Moreover, Jiang et al. [24] used epoxy as the main raw material in FDM technique to get the best use of its mechanical properties and print products that can be used in harsh conditions. Tensile specimens were printed of a mixture of only epoxy and CNT giving a tensile strength of 55 MPa.

In this paper, ABS tensile specimens are printed with printing parameters based on the survey presented in Table 1. A comparison between the results of many previous studies is held to decide on the best parameters to print with. Also, using these printing parameters, other tensile specimens are printed to test a new filling technique. This technique is a post processing technique that aims to improve the mechanical properties and reduce cost and weight. Hence, the parts are printed with inner voids which reduce the part's weight, printing time, and in turn printing cost. Afterwards, these voids are injected with low-cost, less dense resin which possesses higher mechanical properties. To make the part sparse inside, voids could be designed and located precisely during design stage by CAD software, or by slicing software which manages this process through infill density parameter [29]. In this study, the parts are made sparse by slicing software, three infill densities are printed (20%, 40%, and 60%) and injected with epoxy resin that is 91% cheaper than the ABS material. The infill pattern chosen is gyroid pattern in order to let the resin spread through the entire part. Tensile tests and morphology analysis are performed to investigate the improvement of this technique.

2 Experimental

2.1 Materials and samples

In this study, ABS (acrylonitrile butadiene styrene) had been used as a filament material; it was obtained from

Table 2 Physical and chemical properties for Deco-pox039

Property	Resin	Hardener
Boiling point/boiling range	>200 °C	>200 °C
Flash point	>150 °C	>100 °C
Density at 23 °C	Approximately 1.1 g cm^{-3}	Approximately 1.03 g cm^{-3}
Viscosity dynamic at 23 °C	Approximately 1000 MPa s	Approximately 190 MPa s
Density of the mixture at 23 °C	1.1 g cm^{-3}	

(AMTech 3D Printing company, Cairo, Egypt) with a 2.85-mm diameter, 1.1 g cm^{-3} density, and 41 g/10 min metal flow index. Deco-pox 039 epoxy resin was obtained from (Pioneers for Polymers & Chemicals PPC company, Alexandria, Egypt). The resin has a bisphenol-A base, and the hardener has polyamine one [30]. Table 2 shows the resin properties.

Tensile specimens were designed according to ASTM638 type I [31], and printed on Ultimaker[3] with nozzle diameter 0.4 mm and Cura 4.8 slicing software in ideaspace company as shown in (Fig. 1).

2.2 Methodology

2.2.1 Printing 100% infill specimens

In this study, 100% infill ABS tensile specimens were printed with printing parameters that were precisely selected based on the literature in Table 1; the selected parameters are believed to give the best results as they were selected based on the previous experimental work done on this material regarding the results obtained in every study. Table 3 summarizes the parameters used in the present study. After printing, tensile test was performed, and all tensile tests in this research had been performed on German Zwick testing machine Z010.

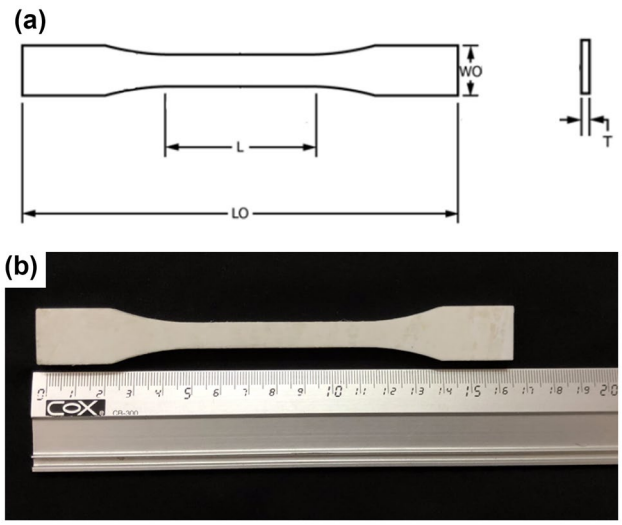

Fig. 1 Specimen geometry according to ASTM D638 standard (**a**) and printed tensile specimen (**b**)

2.2.2 Filling technique

In this technique, tensile specimens were printed with inner voids to be injected with epoxy resin. ABS specimens were sparse inside using the slicing software. The software controls how dense the part is by infill percentage parameter. Three percentages were printed 20%, 40%, and 60% with a pattern that allowed the resin to flow through the whole specimen, and two holes of 0.4 mm for injection and venting were drilled in the specimens (Fig. 2).

To identify the mechanical properties of the epoxy resin being used, tensile test was done on deco-Pox039 Epoxy resin, two components A and B were mixed together under the predefined percentages, then the mix was poured into a custom-made silicone rubber mold in (Fig. 3a) and was let for 7 days to complete the full curing as written in the product data sheet; the test was done following ASTM638 type I.

After testing the epoxy specimens and confirming its properties, it was approved to be used as an injection material. Epoxy injection within the ABS printed tensile specimens was done using a syringe. The syringe was immersed inside the specimen through one of the holes and was sealed very well. The other hole was for venting. The syringe used was G16 to suit the highly viscous epoxy. The injection process was in vertical orientation, the syringe was immersed at the bottom, and the direction of the injection was against gravity

Table 3 Printing parameters for ABS

Printing temperature	240 °C
Printing speed	40 mm s^{-1}
Layer thickness	0.2 mm
Build plate temperature	100 °C
Printing orientation	Horizontal
Raster angle	0°
Infill pattern	Lines

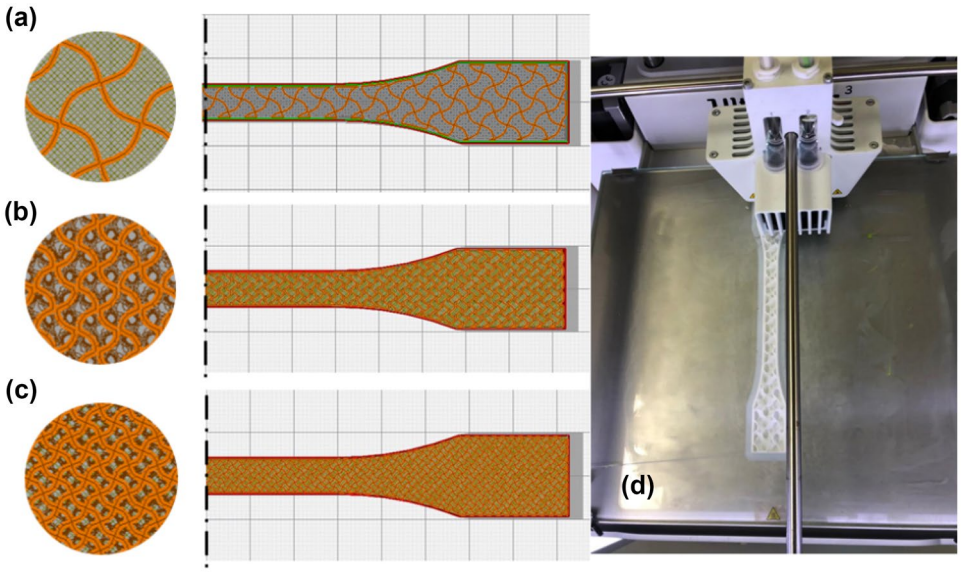

Fig. 2 20% infill ABS tensile specimen (**a**), 40% infill ABS tensile specimen (**b**), 60% infill ABS tensile specimen (**c**), and 20% infill ABS specimen while printing on Ultimaker[3] (**d**)

to make sure the epoxy filled the whole specimen by reaching the top. Figure 4 shows the direction of injection. Figure 5 represents sections at different locations in a specimen to make sure that epoxy flowed through the whole specimen. A tensile test was done — after 7 days from the injection of specimens, the full curing time — on German Zwick testing machine Z010, with 10 KN calibrated load cell, and crosshead speed of 5 mm min^{-1}. At least three samples for each case were tested. Morphology analysis on the fractured specimens had been done, as the fracture surfaces were observed via scanning electron microscope (SEM, JEOL JSM_5400LV). All the surfaces were gold-sputtered before observation, and the observation was at an acceleration voltage of 15 kV.

3 Results and discussion

3.1 Results of epoxy resin test

The mechanical behavior of deco-Pox039 Epoxy resin is shown in (Fig. 6); the tensile test was done on four specimens to take the average and give the most accurate result. The epoxy used in this paper has a resin of aromatic bisphenol (bisphenol-A) and a hardener of amino methylamine and phenyl methylamine. The ultimate tensile strength obtained was 44.8 ± 1.1 MPa, and elongation at break was of 10.3 ± 0.03%. This result is higher than the tensile strength obtained by Filippova et al. [25], and

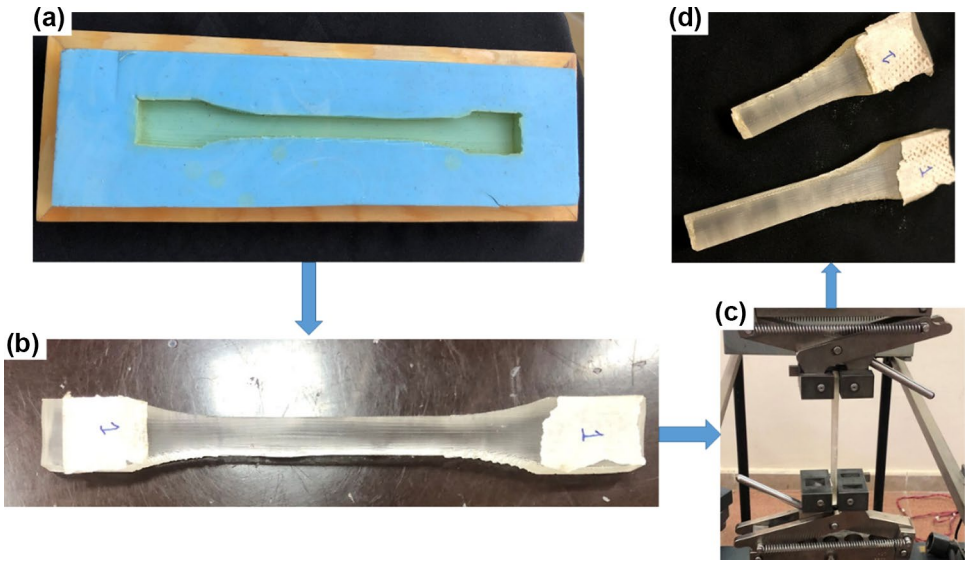

Fig. 3 Epoxy set: Silicon mold for casting epoxy (**a**), casted epoxy tensile specimen (**b**), epoxy specimen during testing (**c**), and epoxy specimen after break (**d**)

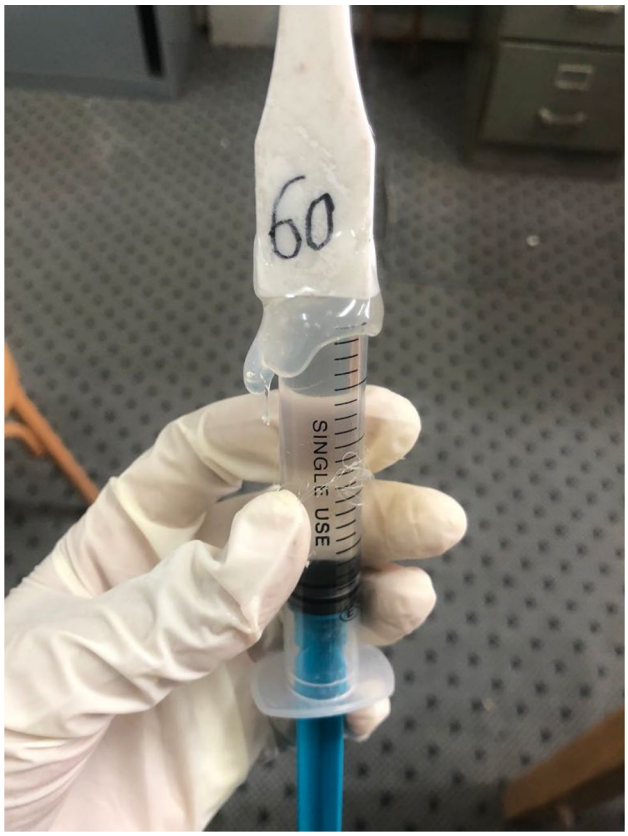

Fig. 4 Injection process of 60% infill tensile specimen

it is related to the chemical composition, since the hardeners tested by Filippova et al. were triethylenetetramine (TETA) and polyethylene polyamine (PEPA) which resulted in tensile strength of 22.4 MPa and 22.7 MPa, respectively. On the other hand, Halder et al. [32] used a resin of bisphenol-A and amine-based hardener so their results were very close to the results in this paper as they recorded 41.92 MPa as best tensile strength. Agarwal and Agarwal [33] tested the bisphenol-A resin with two different hardener types: triethylenetetramine (TETA) and diaminodiphenyl methane (DDM) giving a strength of 52 MPa and 83 MPa, respectively. And when using bisphenol-F as a resin with aromatic amine hardener, the strength reached 84 MPa [34].

3.2 Results of 100% infill ABS test

Figure 7 represents the result of the tensile test on 100% infill printed ABS specimens with the parameters in Table 3. Three specimens were tested, elongation at break was 7.4%, and tensile strength was 36.3 ± 0.81 MPa. This result is considered one of the best results obtained for 100% infill ABS tensile specimens. Figure 8 shows a comparison between the result of the present study, and most of the results obtained in the studies mentioned in Table 1. The variation in results

Fig. 5 Sections in injected tensile specimen (**a**); top view of the sections (**b**)

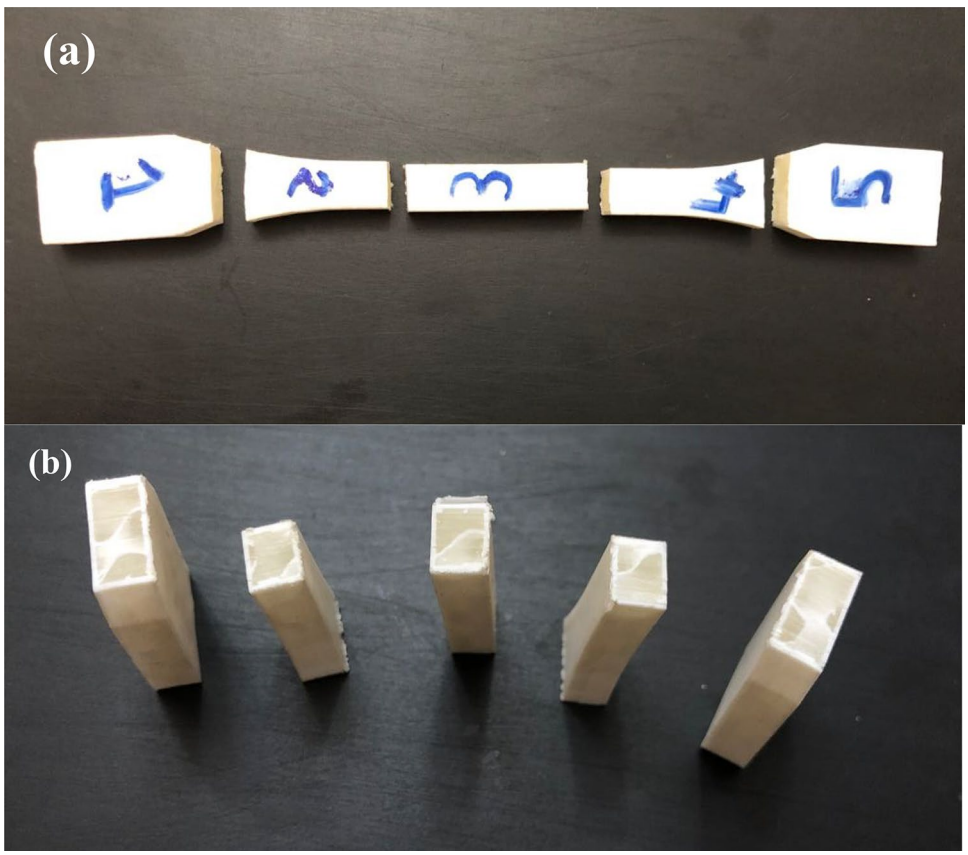

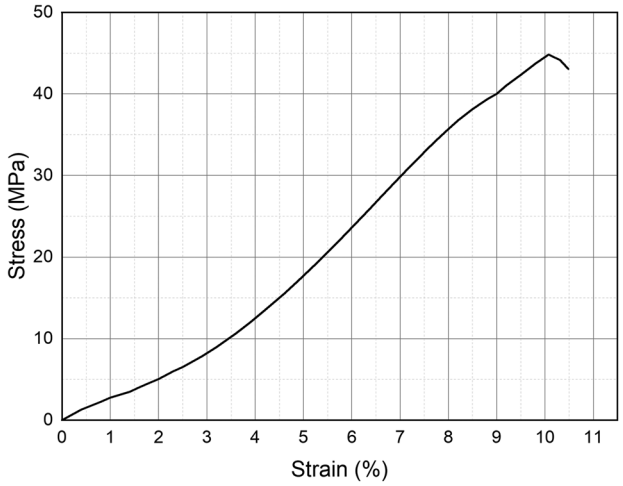

Fig. 6 Deco-pox039 average tensile test result

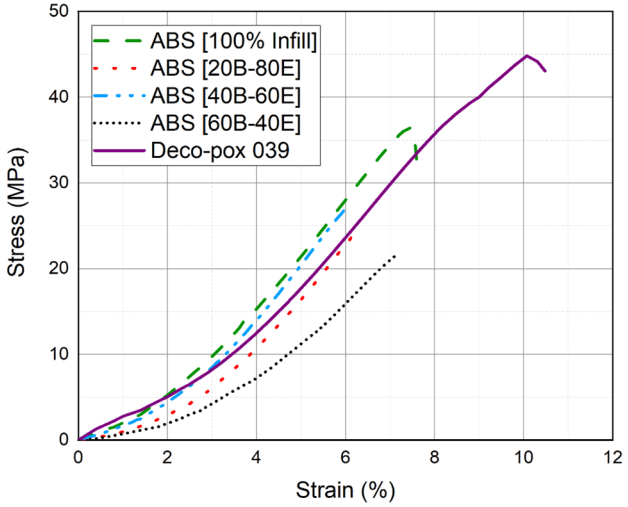

Fig. 9 Results of composition technique in 20%, 40%, and 60% infill in comparison with 100% ABS infill

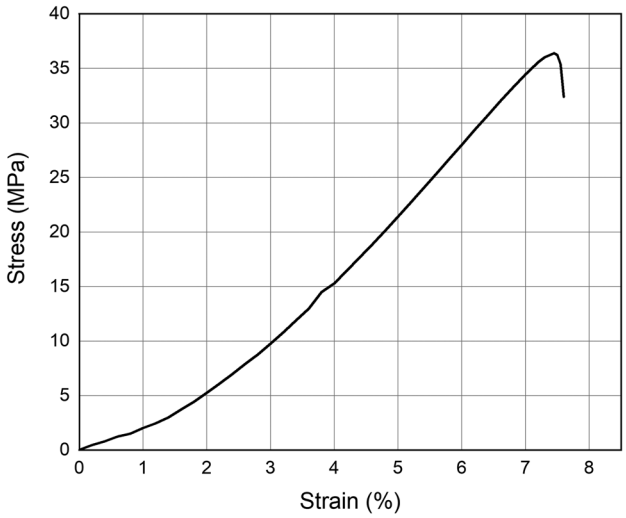

Fig. 7 Results of ABS 100% infill tensile test

ensures the influence of printing parameters on the mechanical properties of the printed part. Table 4 compares the printing parameters used in the present study to those used by T. Coogan and Kazmer [16] as they got the closest results to this study's results. Both studies have very close parameters. The main difference is in layer height parameter as 0.2 mm layer height adopted in this research is believed to be the best height fulfilling the best boding between adjacent roads and consecutive layers [35, 36].

3.3 Results of filling ABS test

The effect of epoxy resin injection within ABS printed parts is represented in (Fig. 9). All printing parameters, injection materials, and methods were controlled; the variables were the infill density of ABS while printing, and in turn the injected volume of epoxy.

Fig. 8 Tensile strength values reported by other researchers for 100% infill ABS compared with the obtained one by present study

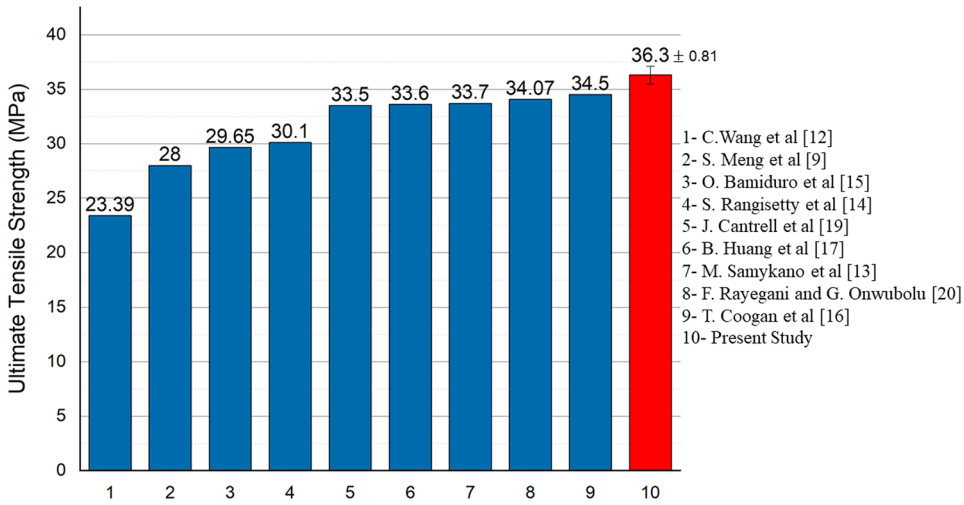

Table 4 Comparison between printing parameters in the present study and in the nearest paper to this paper's result

	Present study (tensile strength: 36.3 MPa)	Coogan et al. [16] (tensile strength: 34.5 MPa)
Printing temperature	240 °C	80 °C
Bed temperature	100 °C	125 °C
Printing speed	40 mm s^{-1}	2000 mm min^{-1} ≅ 33.33 mm s^{-1}
Layer height	0.2 mm	0.3 mm
Pattern	Lines	Lines
Raster angle	0 °	0°

Table 5 Physical and mechanical properties obtained from ABS test

	Ultimate tensile strength (MPa)	Strain at ultimate strength (%)	Printing time	Printed weight (g)	Printed weight reduction (100%)	Strength/printed weight ratio	Specimen weight (g)
100% ABS infill	36.30	7.40	1 h 36 m	16	0%	2.32	16
20% ABS infill	24.77	6.27	59 m	7	56.25%	3.50	16
40% ABS infill	27.03	6	1 h 8 m	9	43.75%	3	16
60% ABS infill	21.80	7.20	1 h 29 m	12	25%	1.80	16

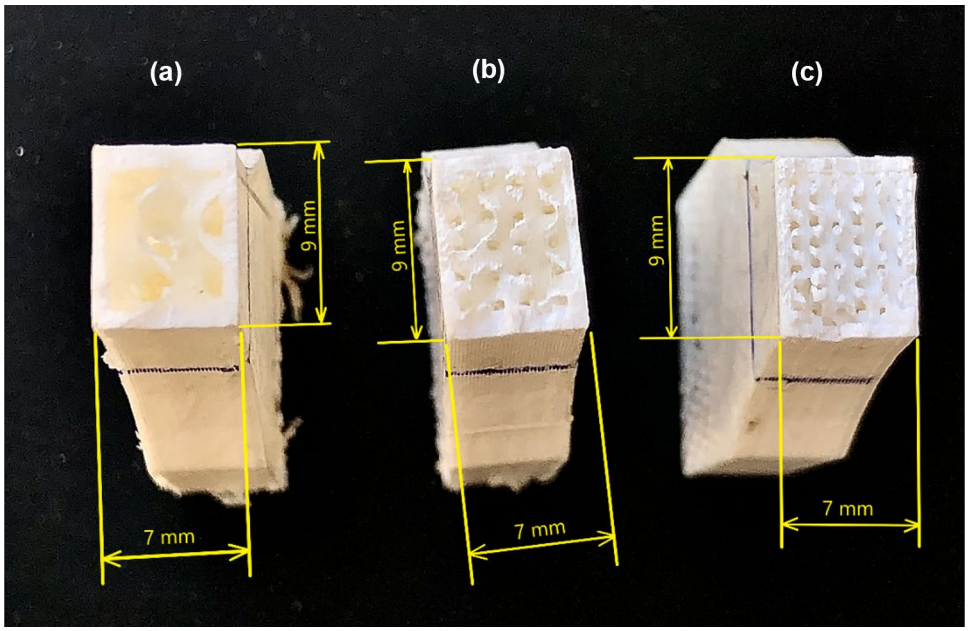

Fig. 10 Sections in tested injected ABS specimens with infill: 20% (**a**), 40% (**b**), and 60% (**c**)

As can be seen, the results are very close, average tensile strength for 20% ABS infill-80% epoxy injection (**20B-80E**) is 24.77 MPa, for 40% ABS infill-60% epoxy injection (**40B-60E**) is 27.03 MPa, and 21.8 MPa for 60% ABS infill-40% epoxy injection (**60B-40E**). Although the strength of 40% infill is marked the best, by analyzing the weight and corresponding printing time, (**20B-80E**) gave the optimum strength to printed weight ratio Table 5. Furthermore, the preference of 20% infill ABS injected with epoxy to the pure 100% infill printed ABS was investigated, and it was concluded that by reducing 56% of the part weight – in 20% infill —, the product mechanical strength reaches 68% of the printed part with 100% infill, and the strength to printed weight ratio is increased by 151% (Table 5). Strength to printed weight ratio is analyzed in this study rather than the common strength to weight ratio, because the injected epoxy resin has the same density of ABS filament used –1.1 g cm^{-3}. Some other thermoplastic filament materials like PLA which possesses higher density (1.17–1.24 g cm^{-3}) [11] might show better

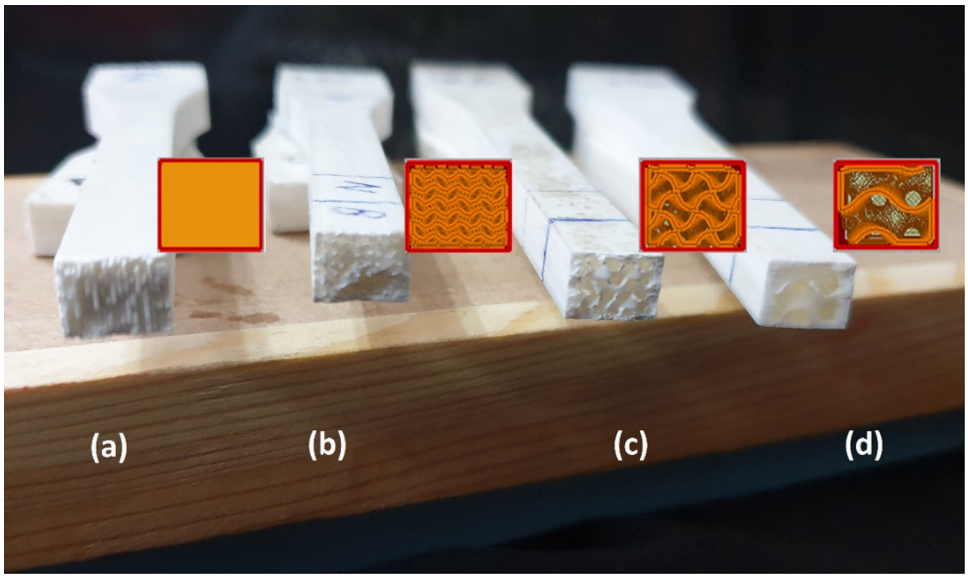

Fig. 11 Sections in the produced parts: 100% infill ABS part **(a)**, epoxy injected 60% infill ABS part **(b)**, epoxy injected 40% infill ABS part **(c)**, and epoxy injected 20% infill ABS part **(d)**

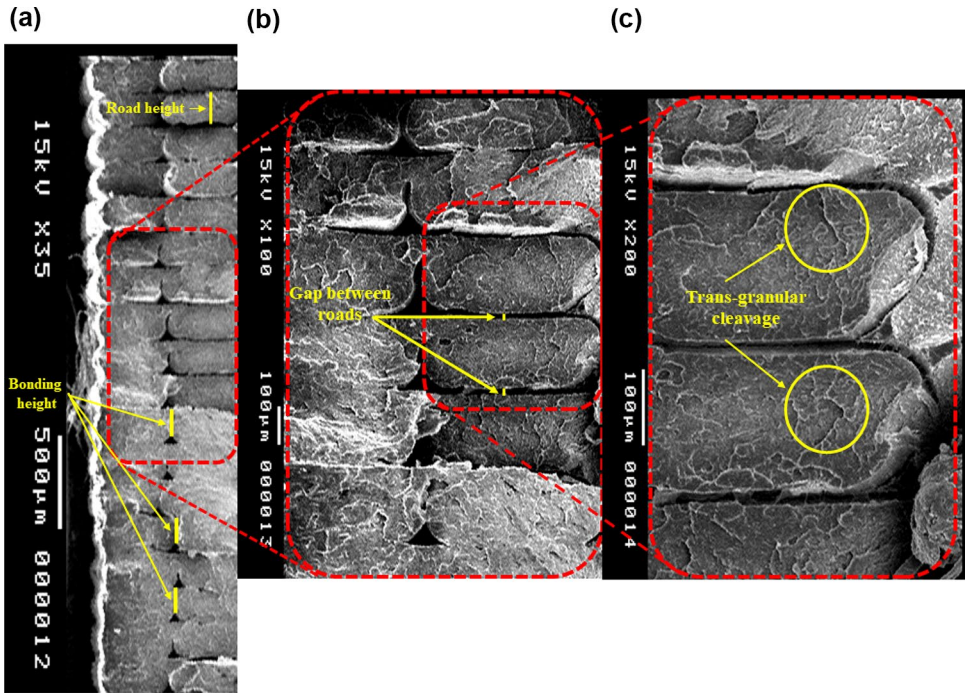

Fig. 12 SEM micrograph of ABS specimens: overview for two adjacent roads in different consecutive layers (**a**), bonding in six consecutive layers (**b**), and the circles indicates the trans-granular cleavage in each road (**c**)

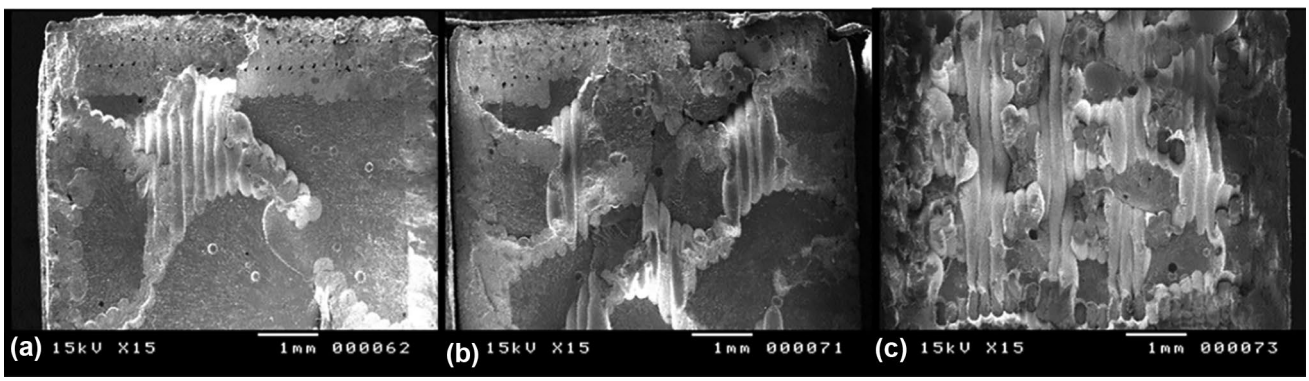

Fig. 13 SEM micrographs for: (**20B-80E**) (**a**), (**40B-60E**) (**b**), and (**60B-40E**) specimens (**c**)

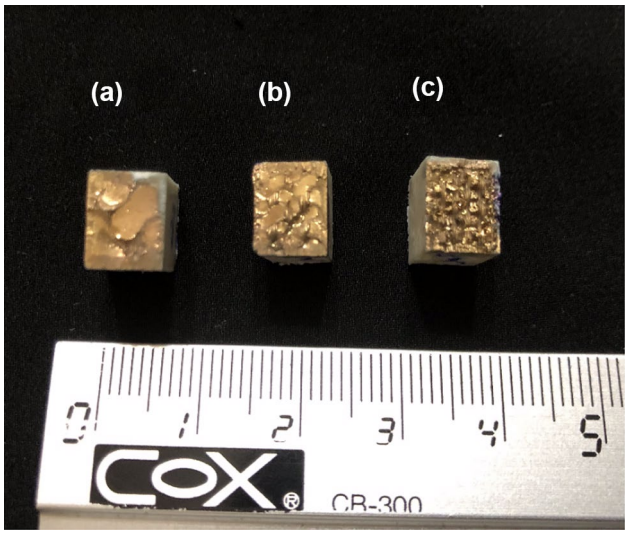

Fig. 14 Coated sections of: (**20B-80E**) (**a**), (**40B-60E**) (**b**), and (**60B-40E**) specimens (**c**)

results when injected with similar epoxy types. Results of the previous tests indicate adequate adhesion between epoxy and ABS. Since the effective surface is considered the main parameter to give best adhesion, and one of the techniques to enhance the effective surface is roughening it but to an acceptable level. As if the surface is more rough the adhesion stress would decrease [37]. And hence one of the themes of FDM process is the moderate surface finish [38, 39], so that would fulfill good adhesion between epoxy and ABS. Figures 10 and 11 represent sections in 20%, 40%, 60%, and 100% infill specimens after injection and testing.

4 Morphology analysis

Results for morphology analysis are shown in Fig. 12; it illustrates the bonding between the adjacent roads of ABS filament in the same layer, and shows the bonding between the consecutive ABS layers. The first remark is that road cross-sections are not circular anymore and that is due to the compression induced from the layers on one another. The bonding between adjacent roads is on more than 50% of its height, when notice the lines in Fig. 12a, it could be concluded that the bonding height is between 90 and 170 µm. The gaps between consecutive layers are represented by lines in Fig. 12b, and the gap height is between 18 to 21 µm. The trans-granular cleavage shown in each road cross-section indicates the brittle fracture mode of the material (Fig. 12c).

Figure 13 shows SEM micrographs of an overview for three sections in (**20B-80E**), (**40B-60E**), and (**60B-40E**) specimens (a, b, and c), respectively. In the micrographs of the injected ABS specimens, the contact surfaces between epoxy and ABS could be marked indicating super adhesion. Small discrete surface areas inside ABS specimens that were designed by printing software helped to make it fully composite as the epoxy was immersed through the whole part (Fig. 14), representing the three coated sections before being examined in the microscope.

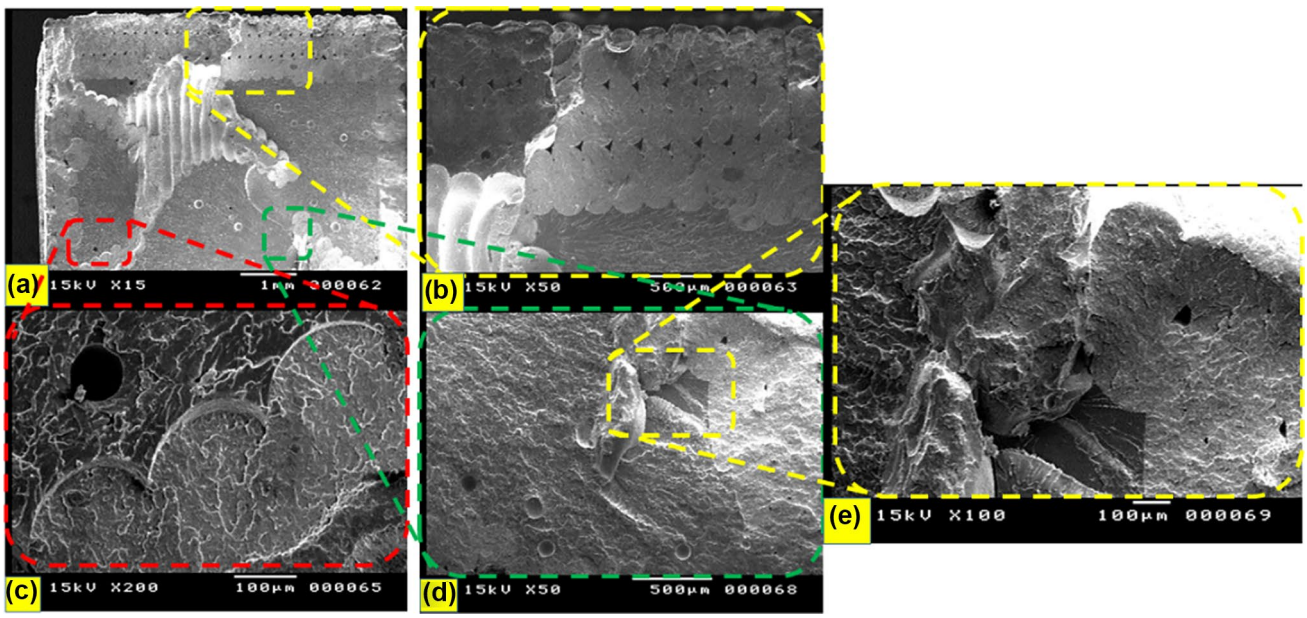

Fig. 15 SEM micrographs in (**20B-80E**) indicate: an overview in the section (**a**), three levels of unpaved fractured surface (**b**), a perfect bond between epoxy and ABS (**c**), the presence of air bubbles (**d**), and beach marks of brittle fracture (**e**)

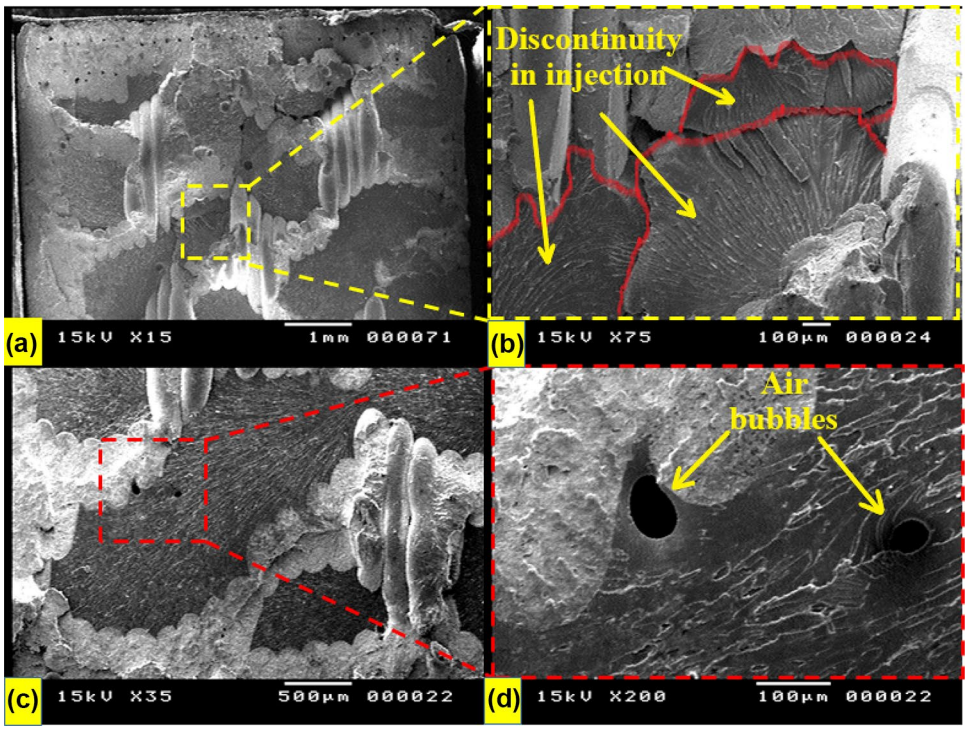

Fig. 16 SEM micrographs in **(40B-60E)** indicate: an overview in the section (**a**), discontinuity in epoxy injection (**b**), two air bubbles in the epoxy mix (**c**), and magnified image of the air bubbles (**d**)

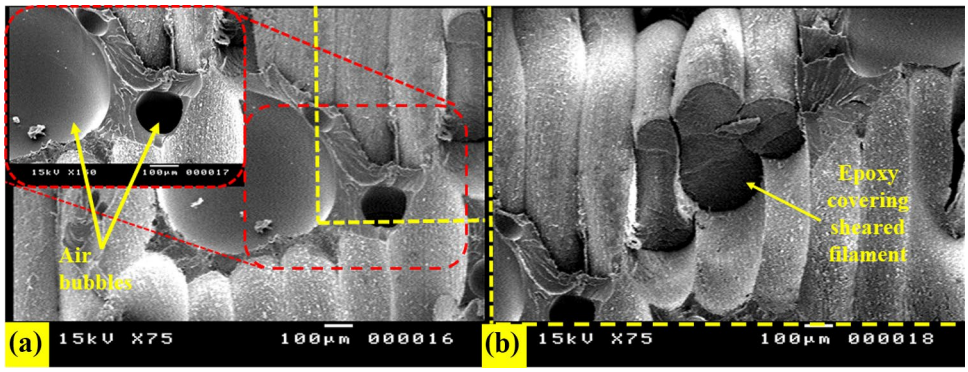

Fig. 17 SEM micrographs in **(60B-40E)** indicate: collapsed air bubble by the fracture (**a**), and epoxy covering some sheared filaments (**b**)

By going deep in (**20B-80E**) specimen (Fig. 15), there are three levels of the ABS road as the mechanical fracture leaves unpaved surface in Fig. 15b; in Fig. 15c, there is a perfect bond between epoxy and ABS with a vital defect in epoxy resin mix indicating some air bubbles; Fig. 15d, e indicate the presence of more air bubbles; beach marks appeared to ensure the brittle fracture; also, different levels of fracture in both epoxy and ABS appeared.

The same phenomena were recognized in Figs. 16 and 17 representing (**40B-60E**) and (**60B-40E**) specimens, respectively. Figure 16b is a magnified image of Fig. 16a where the brittle fracture is obvious, and also, it refers to discontinuity in injection. Figure 16d is a magnified image of Fig. 16c, and it shows 50 and 35 µm air bubbles in epoxy mix (Fig. 17a) representing the fracture; it was just before a relatively large air bubble, and also, there is another one that collapsed by the fracture; Fig. 17b represents epoxy that covers some sheared filaments.

5 Conclusions

Parts printed by FDM technique have some limitations in the mechanical properties. In this study, it was proofed that printing parameters highly affect the tensile strength. ABS tensile specimens were printed by FDM technique and evaluated according to ASTM638 giving one of the best recorded results, with an ultimate strength of 36.3 MPa. Also, this work was devoted to study the effect a new compositing technique on mechanical properties. Parts printed with

different infill densities (20%, 40% and 60%) and injected with epoxy. This technique resulted in an improvement in strength to printed weight ratio by 151% in case of 20% infill and 129% in case of 40% infill specimens, but there was not any significant improvement in case of 60% infill specimens. The improvement in properties is directly proportional to the volumes of the injected material and ABS cavities. As in parts with 20% infill, large cavities allowed the viscous epoxy to fill the entire volume. On the contrary, in 60% infill, cavities were relatively small which justifies the results obtained. Morphology analysis showed good adhesion between epoxy and ABS cavities, with the presence of some air bubbles. Based on the present findings, parts printed with the adopted printing parameters and composited by the presented filling technique could be applied in a wide range of applications.

Author contribution All authors contributed to the study conception and design. Material preparation and data collection were performed by Heba Hussam. Data analysis was performed by Heba Hussam and Yasser Abdelrhman. The first draft of the manuscript was written by Heba Hussam. All authors commented on previous versions of the manuscript. All authors read and approved the final manuscript.

Funding Open access funding provided by The Science, Technology & Innovation Funding Authority (STDF) in cooperation with The Egyptian Knowledge Bank (EKB).

Declarations

Competing interests The authors declare no competing interests.

References

1. Niaki MK, Nonino F (2018) Industries and applications. In: Pham DT (ed) The management of additive manufacturing. Springer, pp 37–66. https://doi.org/10.1007/978-3-319-56309-1
2. Oliveira JP, LaLonde AD, Ma J (2020) Processing parameters in laser powder bed fusion metal additive manufacturing. Mater Des 193:1–12. https://doi.org/10.1016/j.matdes.2020.108762
3. Ramalho A, Santos TG, Bevans B et al (2022) Effect of contaminations on the acoustic emissions during wire and arc additive manufacturing of 316L stainless steel. Addit Manuf. https://doi.org/10.1016/j.addma.2021.102585
4. Shen J, Zeng Z, Nematollahi M et al (2021) In-situ synchrotron X-ray diffraction analysis of the elastic behaviour of martensite and H-phase in a NiTiHf high temperature shape memory alloy fabricated by laser powder bed fusion. Addit Manuf Lett 1:100003. https://doi.org/10.1016/j.addlet.2021.100003
5. Ćwikła G, Grabowik C, Kalinowski K et al (2017) The influence of printing parameters on selected mechanical properties of FDM / FFF 3D-printed parts. ModTech Int Conf Inds Eng. https://doi.org/10.1088/1757-899X/227/1/012033
6. Hanssen J, Moe ZH, Tan D et al (2015) Rapid prototyping in manufacturing. In: Nee AYC (ed) Handbook of manufacturing engineering and technology. Springer, pp 2505–2523. https://doi.org/10.1007/978-1-4471-4670-4
7. Abu M, Khondoker H, Asad A, Sameoto D (2018) Printing with mechanically interlocked extrudates using a custom bi-extruder for fused deposition modelling. Rapid Prototyp J 8(4):248–257. https://doi.org/10.1108/RPJ-03-2017-0046
8. Ngo TD, Kashani A, Imbalzano G et al (2018) Additive manufacturing (3D printing): a review of materials, methods, applications and challenges. Compos Part B Eng 143:172–196. https://doi.org/10.1016/j.compositesb.2018.02.012
9. Meng S, He H, Jia Y et al (2017) Effect of nanoparticles on the mechanical properties of acrylonitrile–butadiene–styrene specimens fabricated by fused deposition modeling. J Appl Polym Sci 134:1–9. https://doi.org/10.1002/app.44470
10. Shojib Hossain M, Espalin D, Ramos J et al (2014) Improved Mechanical Properties of Fused Deposition Modeling-Manufactured Parts Through Build Parameter Modifications. J Manuf Sci Eng 136:061002. https://doi.org/10.1115/1.4028538
11. Yao T, Ye J, Deng Z et al (2020) Tensile failure strength and separation angle of FDM 3D printing PLA material : Experimental and theoretical analyses. Compos Part B 188:107894. https://doi.org/10.1016/j.compositesb.2020.107894
12. Wang CC, Lin TW, Hu SS (2007) Optimizing the rapid prototyping process by integrating the Taguchi method with the Gray relational analysis. Rapid Prototyp J 13:304–315. https://doi.org/10.1108/13552540710824814
13. Samykano M, Selvamani SK, Kadirgama K et al (2019) Mechanical property of FDM printed ABS : influence of printing parameters. Int J Adv Manuf Technol 102:2779–2796. https://doi.org/10.1007/s00170-019-03313-0
14. Rangisetty S, Peel LD (2017) The effect of infill patterns and annealing on mechanical properties of additively manufactured thermoplastic composites. the ASME Conference SMASIS2017–4011. 1–12. https://doi.org/10.1115/SMASIS2017-4011. Accessed 16 Nov 2017.
15. Bamiduro O, Owolabi G, Haile MA, Riddick JC (2019) The influence of load direction, microstructure, raster orientation on the quasi-static response of fused deposition modeling ABS. Rapid Prototyp J 25(3):462–472. https://doi.org/10.1108/RPJ-04-2018-0087
16. Coogan TJ, Kazmer DO (2017) Bond and part strength in fused deposition modeling. Rapid Prototyp J 23:414–422. https://doi.org/10.1108/RPJ-03-2016-0050
17. Huang B, Meng S, He H et al (2018) Study of processing parameters in fused deposition modeling based on mechanical properties of acrylonitrile-butadiene-styrene filament. Polym Eng Sci. https://doi.org/10.1002/pen.24875
18. Koch C, Van Hulle L, Rudolph N (2017) Investigation of mechanical anisotropy of the fused filament fabrication process via customized tool path generation. Addit Manuf 16:138–145. https://doi.org/10.1016/j.addma.2017.06.003
19. Cantrell J, Rohde S, DiSandro L et al (2016) Experimental characterization of the mechanical properties of 3D printed ABS and polycarbonate parts. In:Yoshida S, Lamberti L, Sciammarella C (eds) Advancement of optical methods in experimental mechanics. Springer, 3:89–105. https://doi.org/10.1007/978-3-319-41600-7

20. Rayegani F, Onwubolu GC (2014) Fused deposition modelling (fdm) process parameter prediction and optimization using group method for data handling (gmdh) and differential evolution (de). Int J Adv Manuf Technol 73:509–519. https://doi.org/10.1007/s00170-014-5835-2
21. Zhu D, Ren Y, Liao G et al (2017) Thermal and mechanical properties of polyamide 12 / graphene nanoplatelets nanocomposites and parts fabricated by fused deposition modeling. J Appl polymer Sci 45332:1–13. https://doi.org/10.1002/app.45332
22. Nabipour M, Akhoundi B (2020) An experimental study of FDM parameters effects on tensile strength, density, and production time of ABS/Cu composites. J Elastomers Plast. https://doi.org/10.1177/0095244320916838
23. Jo W, Kwon O, Moon M (2018) Investigation of in fluence of heat treatment on mechanical strength of FDM printed 3D objects. Rapid Prototyp J 24(3):615–622. https://doi.org/10.1108/RPJ-06-2017-0131
24. Jiang Q, Zhang H, Rusakov D, Bismarck A (2021) Additive manufactured carbon nanotube/epoxy nanocomposites for heavy-duty applications. ACS Appl Polym Mater. https://doi.org/10.1021/acsapm.0c01011
25. Filippova AV, Lopatina YA, Sviridov AS (2021) Study of the tensile strength of a polymer composite material based on ABS-plastic and impregnated in epoxy resin with different types of hardener: study of the tensile strength of a polymer composite material based on ABS-plastic and impregnated in epoxy. https://doi.org/10.1088/1742-6596/1990/1/012015
26. Gao C, Yu T, Sun J et al (2021) A phosphate covalent organic framework: synthesis and applications in epoxy resin with outstanding fire performance and mechanical properties. Polym Degrad Stab 190:109613. https://doi.org/10.1016/j.polymdegradstab.2021.109613
27. Kasper Y, Albiez M, Ummenhofer T et al (2021) Application of toughened epoxy-adhesives for strengthening of fatigue-damaged steel structures. Constr Build Mater 275:121579. https://doi.org/10.1016/j.conbuildmat.2020.121579
28. Chang W, Rose LRF, Islam MS et al (2021) Strengthening and toughening epoxy polymer at cryogenic temperature using cupric oxide nanorods. Compos Sci Technol 208:108762. https://doi.org/10.1016/j.compscitech.2021.108762
29. Belter JT, Dollar AM (2015) Strengthening of 3D printed fused deposition manufactured parts using the fill compositing technique. PLoS ONE. https://doi.org/10.1371/journal.pone.0122915
30. Deco-Pox 039 (MSDS) 1
31. E3-95 (2016) Standard practice for preparation of metallographic specimens. ASTM Int 82:1–15. https://doi.org/10.1520/D0638-14.1
32. Halder S, Ghosh PK, Goyat MS, Ray S (2013) Ultrasonic dual mode mixing and its effect on tensile properties of SiO_2-epoxy nanocomposite. J Adhes Sci Technol. https://doi.org/10.1080/01694243.2012.701510
33. Agarwal KK, Agarwal G (2019) a study of mechanical properties of epoxy resin in presence of a study of mechanical properties of epoxy. Conference: Technological Innovation In Mechanical Engineering
34. Bajpai A, Wetzel B (2019) Tensile testing of epoxy-based thermoset system prepared by different methods. 1–8. https://doi.org/10.20944/preprints201907.0143.v1
35. Luzanin O, Movrin D, Guduric V (2019) Impact of processing parameters on tensile strength, in-process crystallinity and mesostructure in FDM-fabricated PLA specimens. Rapid Prototyp J 8:1398–1410. https://doi.org/10.1108/RPJ-12-2018-0316
36. Vishwas M, Basavaraj CK (2017) Studies on optimizing process parameters of fused deposition modelling technology for ABS. Mater Today Proc 4:10994–11003. https://doi.org/10.1016/j.matpr.2017.08.057
37. Bürenhaus F, Moritzer E, Hirsch A (2019) Adhesive bonding of FDM-manufactured parts made of ULTEM 9085 considering surface treatment, surface structure, and joint design. Weld World 63(6):1819–1832
38. Heshmat M, Abdelrhman Y (2021) Improving surface roughness of polylactic acid (PLA) products manufactured by 3D printing using a novel slurry impact technique. Rapid Prototyp J 27:1791–1800. https://doi.org/10.1108/RPJ-09-2020-0227
39. Abdelaal O, Heshmat M, Abdelrhman Y (2020) Experimental investigation on the effect of water-silica slurry impacts on 3D-Printed polylactic acid. Tribol Int 151:106410. https://doi.org/10.1016/j.triboint.2020.106410